



# Quasi-automatic 3D reconstruction of the full spine from low-dose biplanar X-rays based on statistical inferences and image analysis

Laurent Gajny<sup>1</sup> · Shahin Ebrahimi<sup>1</sup> · Claudio Vergari<sup>1</sup> · Elsa Angelini<sup>2,3</sup> · Wafa Skalli<sup>1</sup>

Received: 6 March 2018 / Accepted: 24 October 2018 / Published online: 31 October 2018  
© Springer-Verlag GmbH Germany, part of Springer Nature 2018

## Abstract

**Purpose** To design a quasi-automated three-dimensional reconstruction method of the spine from biplanar X-rays as the daily used method in clinical routine is based on manual adjustments of a trained operator and the reconstruction time is more than 10 min per patient.

**Methods** The proposed method of 3D reconstruction of the spine (C3–L5) relies first on a new manual input strategy designed to fit clinicians' skills. Then, a parametric model of the spine is computed using statistical inferences, image analysis techniques and fast manual rigid registration.

**Results** An agreement study with the clinically used method on a cohort of 57 adolescent scoliotic subjects has shown that both methods have similar performance on vertebral body position and axial rotation (null bias in both cases and standard deviation of signed differences of 1 mm and 3.5° around, respectively). In average, the solution could be computed in less than 5 min of operator time, even for severe scoliosis.

**Conclusion** The proposed method allows fast and accurate 3D reconstruction of the spine for wide clinical applications and represents a significant step towards full automatization of 3D reconstruction of the spine. Moreover, it is to the best of our knowledge the first method including also the cervical spine.

**Graphical abstract** These slides can be retrieved under electronic supplementary material.

The graphical abstract consists of three slides from a presentation. The first slide, titled 'Key points', lists three points: 1. 3D reconstruction of the spine from biplanar X-rays is a clinically used tool. 2. The strong operator dependency and reconstruction time (≥ 10 min in clinical practice) of the clinically used method limits wide applications. 3. We propose a novel quasi-automated method based on a soft manual intervention, statistical inferences and image analysis techniques. The second slide, titled '3D reconstruction of the spine: retroprojection on the radiographs and 3D output', shows two biplanar X-rays on the left, a 3D reconstruction of the spine in the middle, and a top view of the 3D reconstruction on the right. The third slide, titled 'Take Home Messages', lists three messages: 1. A 3D reconstruction of the spine including cervical vertebrae (C3–C7) can be assessed in less than 5 min by a trained operator. 2. Lower and more intuitive manual intervention for model adjustment. 3. The obtained vertebrae position and axial rotation are close to the range of uncertainty of the clinically used method. Each slide includes the 'Spine Journal' logo and the Springer logo at the bottom.

**Keywords** Scoliosis · 3D reconstruction · Statistical inferences · Landmark detection · Biplanar X-rays

## Introduction

Pathologies of the spine such as adolescent idiopathic scoliosis (AIS) are three-dimensional deformities that affect position and orientation of vertebrae in space [1]. Methods providing 3D reconstructions of the spine allow the quantitative assessment of the deformity, the objective assessment of treatment effect [2, 3], the detection of progressive scoliosis [4] and the surgical planning and simulation [5]. Moreover, the interest

**Electronic supplementary material** The online version of this article (<https://doi.org/10.1007/s00586-018-5807-6>) contains supplementary material, which is available to authorized users.

✉ Laurent Gajny  
Laurent.GAJNY@ensam.eu

Extended author information available on the last page of the article

of considering these deformities from head to pelvis has been demonstrated [6, 7].

Computed tomography (CT) is considered a gold standard for 3D reconstructions, using various segmentation algorithms (see, for instance, [8]). However, these acquisitions cause high ionizing radiations exposure [9], and therefore, they are not appropriate for children with repetitive follow-up examinations. Furthermore, the patient lies in supine position which considerably affects the spine configuration [10]. Alternatively, biplanar X-rays systems providing frontal and lateral views at a lower radiation dose level and in weight-bearing position are increasingly used for spine imaging [11].

Semi-automated 3D reconstruction methods of the thoracolumbar spine from biplanar X-rays have considerably evolved in the last decades, reducing the requested operator time and improving accuracy. An original method relying on the manual identification of the spinal curve and a very few set of landmarks has been proposed in [12], allowing fast generation of a first solution for the 3D reconstruction using a statistical parametric model. After manual adjustments of anatomical features in the model, the 3D reconstruction allowed accurate clinical measurements. This method has been extensively validated for mild and severe scoliosis [13–15], and it is, to the best of our knowledge, the only one widely used both in research and in clinical routine. However, the main limitation regarding the clinical daily use is its operator dependency. While endplate digitization is widely used for clinical parameters measurements (Cobb angle, kyphosis, lordosis), feedback from operators and radiology technicians is that manual adjustments of the 3D model remain an issue in daily routine.

Other similar approaches based on reduced digitalized information and statistical models have been developed [16, 17]. Further approaches are aiming to design quasi or fully automatic method based on artificial intelligence [18, 19]. However, these studies are limited to thoracolumbar spine and pelvis while global analysis appears essential to investigate compensatory adaptations not only at the pelvis level [20, 21] but also at the cervical level [6, 22].

The aim of the present study was to develop a quasi-automatic 3D reconstruction method of the spine, from cervical spine to pelvis, reliable and sufficiently fast to be compatible with clinical daily practice. The manual input of the proposed method was designed to be closer to the type of radiographic measurements routinely performed by clinicians, such as Cobb and sagittal angles.

## Materials and methods

### Database

Two hundred and twenty-eight asymptomatic and AIS patients were retrospectively included in the present study. One hundred and seventy-one of them (age range 6–72 years old) were included in the training group for the statistical model, including 106 asymptomatic patients, 21 moderate AIS scoliotic patients (Cobb range 14°–29°) and 44 severe scoliotic patients (Cobb range 31°–93°). On the other hand, 57 patients were included in the validation process (Table 1). All patients underwent low-dose biplanar X-rays (EOS system, EOS Imaging, Paris, France).

Full 3D reconstructions integrating the lower cervical and thoracolumbar spine were performed for all patients by experienced operators using the previous method [12] and an extension of it for cervical spine reconstruction (C3–C7) [23]. For each subject of the training database, a set of parameters already described in [12] was calculated, to which vertebral endplates orientations were added. Patient inclusions were validated by the Ethical Committee (C.P.P. Ile de France VI).

A previously described in vitro database of dry thoracic and lumbar vertebrae was scanned with CT or physical contact measurement to obtain their 3D geometry [12]. Abnormal vertebrae were excluded, and the database was completed by 27 cervical spines. In total, 1285 vertebrae were measured.

### Manual identifications by a trained user

The user mainly digitalized vertebral endplates on traditional 2D views (Fig. 1). On the sagittal view, the operator identified the upper endplate of C7, the lower endplate of T12 and the sacral endplate. On the frontal view, the operator identified the sacral endplate, helped by a tool displaying the epipolar lines. According to the spinal deformity in the frontal plane, the operator also digitalized endplates corresponding to the 2D Cobb angles (two endplates for a single curvature and three for a double curve). In addition, the operator was asked to identify the odontoid and the acetabula on both views. Based on these identifications, an interactive spinal midline was provided to the user, who could adjust it on both views to make it pass through the centres of all vertebral endplates.

**Table 1** Description of the in vivo testing database

| Agreement                                  | Number | Age mean [min max] | Cobb mean [min max] |
|--|--------|--------------------|---------------------|
| Scoliotic with Cobb angles $\leq 30^\circ$ | 41     | 13 [10–15]         | 18° [10°–29°]       |
| Scoliotic with Cobb angles $> 30^\circ$    | 16     | 14 [10–17]         | 49° [33°–63°]       |

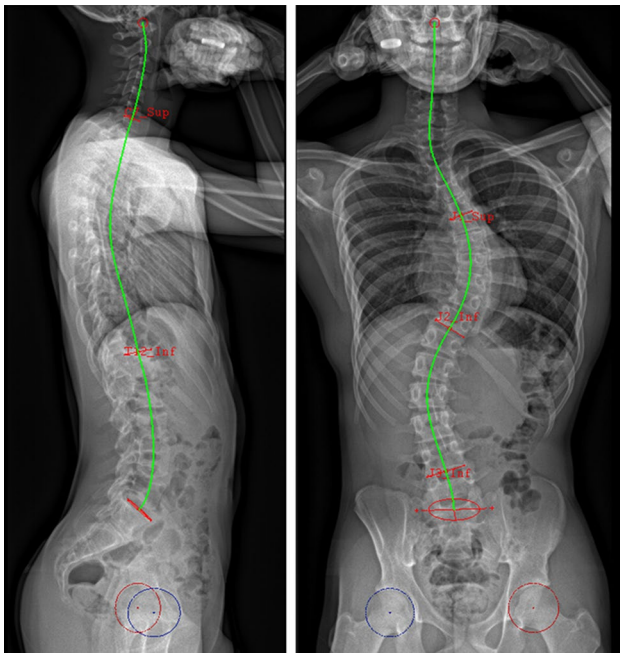


Fig. 1 Manual identifications

### Estimation of the vertebrae position and orientation

From these two 2D curves, a 3D curve was reconstructed to approximate the spinal midline from the sacrum to the odontoid. The longitudinal inferences previously described in [12] have been adapted to estimate the positions of all vertebral endplates along the 3D spinal curve, their depth, width and orientations, thanks to the previously digitized endplates. The manually identified data were used as predictive parameters to determine the whole set of parameters using the a priori knowledge provided by the in vivo training database and Gaussian process regression [24]. The regression method is iterative and it self-improves the model as the algorithm automatically decides to which vertebrae the digitalized endplates belong to. Moreover, lumbar and cervical vertebral corners and visible thoracic endplates were detected automatically and accurately using image processing [25] and machine learning (see Fig. 2). The obtained pieces of information enabled to compute new predictors that again improved the model. At the end of this process, a simplified parametric model of the spine consisting of ellipses representing the endplates was computed.

### Estimation of the vertebrae shape

For each vertebra, transversal inferences from the in vitro database were used to estimate the 3D geometrical vertebral

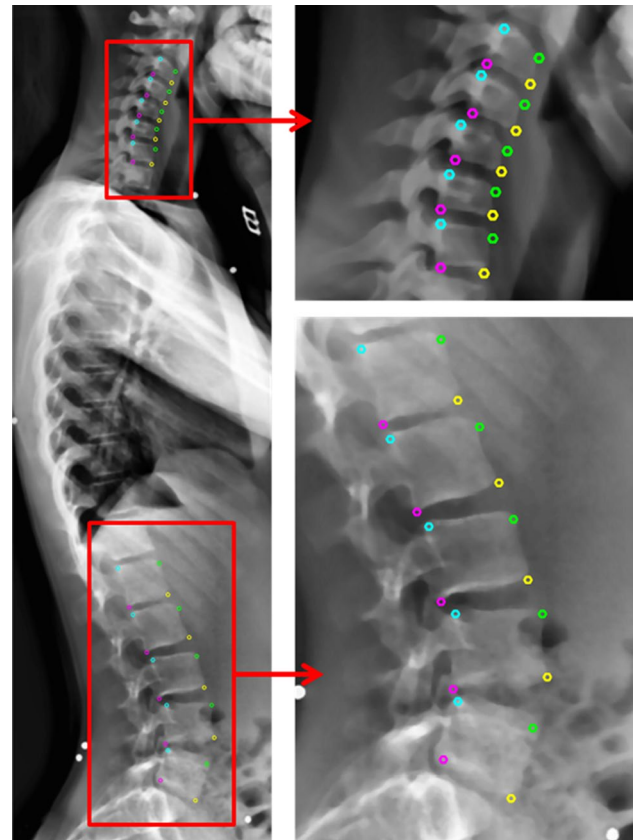
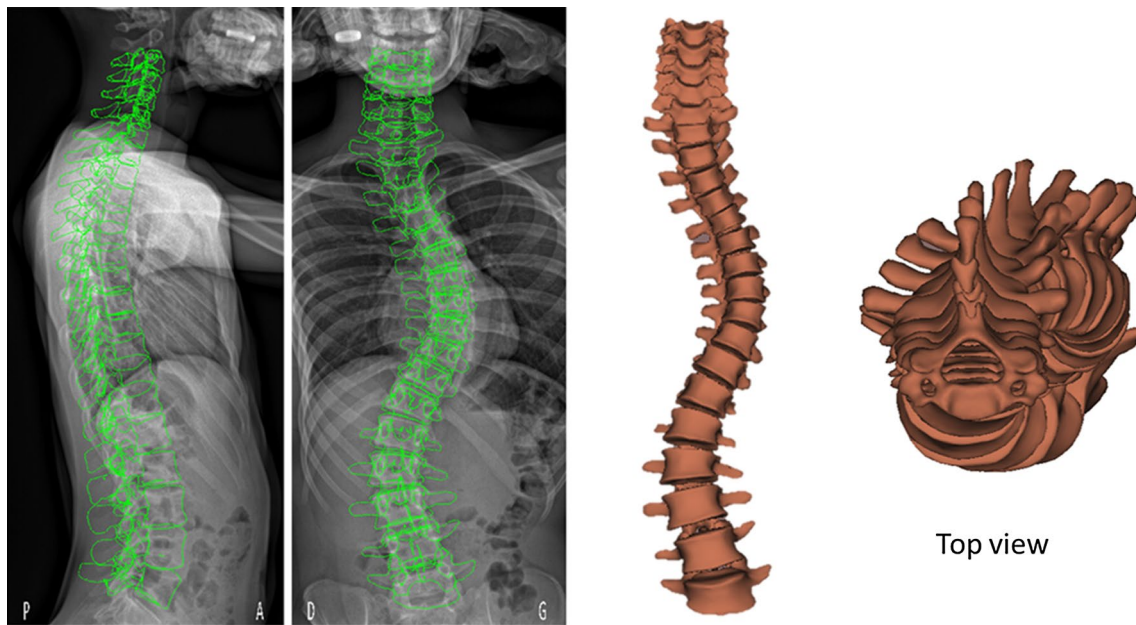


Fig. 2 Automatic corner detection using the method presented in [25]

shape. The method previously proposed in [12] has been adapted to take the lower cervical spine into account. Finally, the operator had the opportunity to refine the model through manual rigid registration of the vertebrae. An example of final output of this reconstruction method is illustrated in Fig. 3.

### Evaluation

Reconstructions obtained by the presented algorithm were compared to the ones obtained with the previous method [12] on the testing set of 57 AIS patients. For each vertebra of each reconstruction, a vertebral frame was computed. Hence, vertebrae positions and orientations could be compared. Table 2 summarizes the signed mean errors and standard deviations (SD) of vertebrae position ( $X$ —antero-posterior,  $Y$ —lateral,  $Z$ —vertical) and orientations (lateral, sagittal, axial). Agreement on spine clinical indices (Cobb angle, axial vertebral rotation at the apex (AVR), T1T12 kyphosis, L1L5 and L1S1 lordosis) and pelvic parameters (pelvic tilt, pelvic incidence and sacral slope) was also considered (Tables 3 and 4, respectively).



**Fig. 3** 3D reconstruction of the spine: retroprojection on the radiographs and 3D output

**Table 2** Evaluation of the agreement between the proposed method and [12] with signed differences (mean ± SD) for position (*X* anteroposterior, *Y* lateral, *Z* vertical) and orientation (*L* lateral, *S* sagittal, *A* axial)

|            | <i>X</i> (mm) | <i>Y</i> (mm) | <i>Z</i> (mm) | <i>L</i> (°) | <i>S</i> (°) | <i>A</i> (°) |
|------------|---------------|---------------|---------------|--------------|--------------|--------------|
| Cobb ≤ 30° |               |               |               |              |              |              |
| Cervical   | 0.5 ± 0.4     | -0.0 ± 1.7    | -0.1 ± 0.6    | -0.1 ± 3.8   | -1.6 ± 4.2   | 0.7 ± 2.1    |
| Thoracic   | 0.4 ± 1.1     | 0.0 ± 1.1     | 0.1 ± 1.1     | 0.0 ± 2.9    | 0.4 ± 2.9    | 0.1 ± 3.7    |
| Lumbar     | 0.9 ± 0.8     | 0.7 ± 1.2     | -0.5 ± 0.9    | 0.3 ± 3.9    | 1.9 ± 3.3    | 0.3 ± 2.8    |
| Cobb > 30° |               |               |               |              |              |              |
| Cervical   | 0.6 ± 0.5     | 0.0 ± 1.4     | 0.1 ± 0.7     | -0.1 ± 3.9   | -1.3 ± 3.8   | 0.5 ± 2.7    |
| Thoracic   | 0.2 ± 1.5     | 0.2 ± 1.6     | 0.3 ± 1.4     | -0.5 ± 3.3   | -0.3 ± 3.5   | 0.4 ± 5.5    |
| Lumbar     | 0.6 ± 1.0     | 0.2 ± 1.6     | -0.6 ± 1.4    | 0.7 ± 4.8    | 2.0 ± 4.6    | 0.4 ± 4.2    |
| All        |               |               |               |              |              |              |
| Cervical   | 0.5 ± 0.4     | -0.0 ± 1.6    | -0.0 ± 0.6    | -0.2 ± 3.9   | -1.5 ± 4.1   | 0.7 ± 2.3    |
| Thoracic   | 0.3 ± 1.2     | 0.1 ± 1.3     | 0.2 ± 1.2     | -0.1 ± 3.1   | 0.3 ± 3.1    | 0.0 ± 4.2    |
| Lumbar     | 0.8 ± 0.9     | 0.3 ± 1.3     | -0.5 ± 1.0    | 0.4 ± 4.2    | 2.0 ± 3.7    | 0.3 ± 3.2    |
| All        | 0.5 ± 1.0     | 0.1 ± 1.4     | -0.0 ± 1.1    | -0.0 ± 3.5   | 0.3 ± 3.7    | 0.2 ± 3.7    |

**Table 3** Evaluation of the agreement between the proposed method and [12] with signed differences (mean ± SD) for spinal clinical parameters

|            | Cobb (°)  | AVR apex (°) | <i>K</i> -T1T12 (°) | <i>L</i> -L1L5 (°) | <i>L</i> -L1S1 (°) |
|------------|-----------|--------------|---------------------|--------------------|--------------------|
| Cobb ≤ 30° | 1.5 ± 4.9 | 1.0 ± 3.5    | 0.2 ± 5.2           | -2.7 ± 5.0         | 0.4 ± 2.8          |
| Cobb > 30° | 3.2 ± 5.8 | 0.4 ± 4.3    | 1.0 ± 6.1           | -4.5 ± 3.2         | 0.1 ± 2.9          |
| All        | 2.0 ± 5.1 | 0.8 ± 3.6    | 0.4 ± 5.4           | -3.2 ± 4.2         | 0.3 ± 2.8          |

**Results**

Mean signed differences of vertebral position between the proposed method and the previous one were lower than 1 mm in all directions, in all vertebral level and

irrespectively of scoliosis severity (Table 2). Standard deviations were lower than 1.6 mm, and 30% of them were lower than 1 mm.

Most of the mean signed orientation differences (78%) were lower than 1° and the remaining ones—which are the mean signed sagittal orientation differences—were lower

**Table 4** Evaluation of the agreement between the proposed method and [12] with signed differences (mean±SD) for spinal clinical parameters

|            | Pelvic tilt | Pelvic incidence | Sacral slope |
|------------|-------------|------------------|--------------|
| Cobb ≤ 30° | -0.1 ± 0.8  | 0.6 ± 1.9        | -0.6 ± 1.9   |
| Cobb > 30° | 0.7 ± 1.0   | 0.3 ± 2.1        | 0.4 ± 2.0    |
| All        | 0.1 ± 0.9   | 0.5 ± 2.0        | -0.4 ± 2.0   |

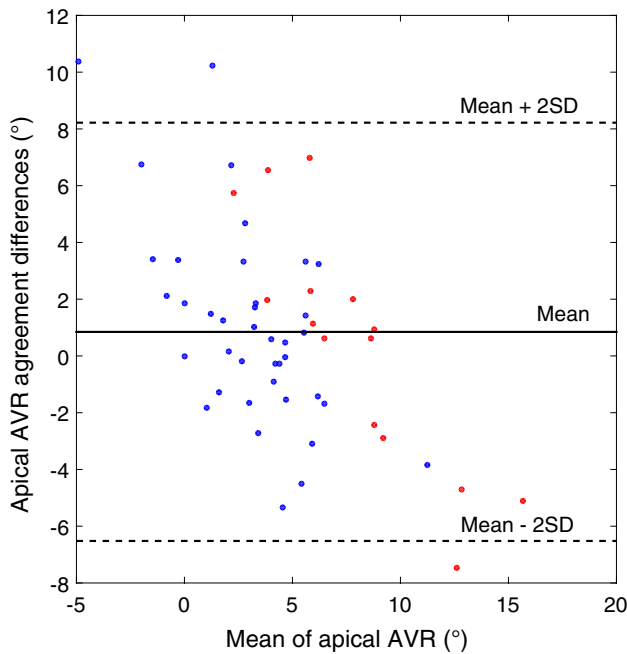


**Fig. 4** Bland–Altman plot for the agreement between the method [12] and the proposed method for axial vertebral rotation of the apical vertebra

than 2°. Standard deviations were mostly lower than 4° and only one exceeded 5° (axial rotation at the thoracic level for severe scoliotic subjects).

Mean differences on spine clinical parameters, described in Table 3, were limited to 1° except for the Cobb angle (lower than 3°) and L1L5 lordosis. Standard deviations

were lower than 6° and in particular lower than 3° for the L1S1 lordosis. Figure 4 shows a Bland–Altman graph for the agreement between the reference and the proposed method for axial vertebral rotation of the apical vertebra.

A similar table is provided for pelvic parameters (Table 4). For all of them, mean differences were no higher than a degree and standard deviation were not exceeding 2°.

Table 5 reports the mean absolute differences (and standard deviations) of vertebral positions and orientation between the current and previous methods, as well as a comparison with a recently published 3D reconstruction algorithm [19] on a cohort of severe scoliotic patients. While the testing datasets were different, mean Cobb angles were similar: 49° in this study and 45° in [19]. With our approach, mean differences were globally similar but smaller than this alternative method, apart from lateral and sagittal vertebral orientations (and consequently, kyphosis and lordosis) where the difference between the two methods did not exceed 1°. Moreover, standard deviations of the differences were systematically lower—of more than 1 mm for position measurements and between 0.8° and 3.2° for angle measurements—with the proposed approach, yielding to lower maximal differences and more reliable reconstructions.

### Discussion and conclusion

Scientific and clinical value of 3D reconstruction of the spine from biplanar X-ray is increasingly confirmed, but complexity and operator dependency of the currently used method in clinical routine is a real limitation to its systematic use. Through a more intuitive initialization process, a combination of automatic and soft manual adjustments, a quasi-automatic method for 3D reconstruction of the spine from biplanar radiographs has been proposed in this study. It is the first one to the best of our knowledge that also includes cervical vertebrae (C3–C7), which can be of great value to characterize compensation mechanisms.

The new identification method was based on standard radiographic identifications. Indeed, orthopaedic surgeons routinely identify junctional vertebrae on frontal

**Table 5** Evaluation of the agreement between the proposed method and [12] on severe scoliotic patients using absolute differences (mean ± SD)

|                        | X (mm)    | Y (mm)    | Z (mm)    | L (°)       | S (°)     | A (°)      |
|------------------------|-----------|-----------|-----------|-------------|-----------|------------|
| This study, Cobb > 30° | 1.0 ± 0.9 | 1.2 ± 1.0 | 0.9 ± 0.9 | 2.8 ± 2.6   | 3.0 ± 2.7 | 3.5 ± 3.1  |
| [19], Cobb > 40°       | 1.5 ± 2.0 | 1.5 ± 2.0 | 1.4 ± 2.6 | 2.7 ± 3.5   | 2.6 ± 3.5 | 4.5 ± 5.8  |
|                        | Cobb (°)  |           | AVR (°)   | K-T1T12 (°) |           | L-L1L5 (°) |
| This study, Cobb > 30° | 4.2 ± 5.0 |           | 3.4 ± 2.4 | 5.2 ± 3.2   |           | 4.9 ± 2.5  |
| [19], Cobb > 40°       | 4.6 ± 6.0 |           | 5.1 ± 5.6 | 4.2 ± 4.9   |           | 4.2 ± 4.9  |

Comparison with the results obtained in [19]

radiographs. Moreover, identifications required on the sagittal view are very similar to classical 2D measurements of thoracic kyphosis and lumbar lordosis. A possible improvement of the method is the full automation of the spinal line adjustment, as it can be challenging for severe scoliosis. When vertebrae are axially rotated, the user has to check that the spinal midline passes through the centre of vertebra endplates and modifies it accordingly. Nonetheless, this identification process was ergonomic and not time-consuming. Indeed, it took less than 2 min 30 per patient (depending on the scoliosis severity) for a trained user.

The automated adjustments proposed in this work—based on statistical inferences, image processing and machine learning—limit the tedious work of adjusting each vertebra manually via elastic deformation. When dealing with scoliotic patients, this step required in the method of [12] took in average more than 10 min for a well-trained user. In the proposed method, faster manual adjustments of the model were possible by rigidly translating and rotating the vertebrae, when necessary. This process took between 1 min 30 and 2 min 30 depending on the scoliosis severity. Therefore, in total, the reconstruction process took less than 5 min per patient, even for severe scoliosis.

The training database was voluntarily constituted of a wide variety of spine morphologies and patient ages. Indeed, the parametric spine representation—taking into account the spinal line curvature, its developed length and some vertebrae dimensions—allows the longitudinal inference model to easily identify whether the patient is young and scoliotic, adult and asymptomatic or every other combination. While this study focused on AIS patients, our method could be then used for a larger population.

Overall, the level of agreement for position between the present method and the previous one [12] was close to the uncertainty range of the latter. Further work should focus on improving the vertebral body and endplates orientation accuracy, although the level of agreement for apical vertebrae axial rotation was close to the uncertainty range documented in [13] for severe scoliosis, which was 6.5°. In this article, the essential pelvic parameters were also considered. As they are computed exactly like in the previous method based on the digitalization of pelvis landmarks [12], we have observed an agreement consistent with the reproducibility study performed in the same article. (For moderate scoliosis, the authors reported an uncertainty of 1.4°, 3.4° and 3.0° for pelvic tilt, pelvic incidence and sacral slope, respectively.) Our approach also offered a better agreement to the previous method than the fully automatic approach described in [19] for vertebrae position, orientation and clinical indices. While a fully automatic method is the target of further research, the proposed method combining automatic adjustments and soft manual intervention constitutes a trade-off between automation and accuracy. Moreover, it contributes to simplify the

process of 3D reconstruction of the spine from head to pelvis. This is essential for a wider application of 3D analysis in clinical routine for diagnosis and treatment planning of scoliosis.

**Acknowledgements** The authors thank the ParisTech BiomecAM chair program, on subject-specific musculoskeletal modelling and in particular Société Générale and COVEA. The authors would also like to thank Aurélien Laville for having initiated this work.

## Compliance with ethical standards

**Conflict of interest** The authors have no conflicts of interest to declare.

## References

1. Stokes IA (1994) Three-dimensional terminology of spinal deformity. A report presented to the Scoliosis Research Society by the Scoliosis Research Society Working Group on 3-D terminology of spinal deformity. *Spine* 19:236–248
2. Ilharreborde B, Sebag G, Skalli W, Mazda K (2013) Adolescent idiopathic scoliosis treated with posteromedial translation: radiologic evaluation with a 3D low-dose system. *Eur Spine J* 22:2382–2391. <https://doi.org/10.1007/s00586-013-2776-7>
3. Illés T, Tunyogi-Csapó M, Somoskeöy S (2011) Breakthrough in three-dimensional scoliosis diagnosis: significance of horizontal plane view and vertebra vectors. *Eur Spine J* 20:135–143. <https://doi.org/10.1007/s00586-010-1566-8>
4. Skalli W, Vergari C, Ebermeyer E et al (2017) Early detection of progressive adolescent idiopathic scoliosis: a severity index. *Spine* 42:823–830. <https://doi.org/10.1097/BRS.0000000000001961>
5. Lafon Y, Steib J-P, Skalli W (2010) Intraoperative three dimensional correction during in situ contouring surgery by using a numerical model. *Spine* 35:453–459. <https://doi.org/10.1097/BRS.0b013e3181b8eaca>
6. Amabile C, Huec J-CL, Skalli W (2016) Invariance of head-pelvis alignment and compensatory mechanisms for asymptomatic adults older than 49 years. *Eur Spine J*. <https://doi.org/10.1007/s00586-016-4830-8>
7. Schwab F, Farcy J-P, Bridwell K et al (2006) A clinical impact classification of scoliosis in the adult. *Spine* 31:2109–2114. <https://doi.org/10.1097/01.brs.0000231725.38943.ab>
8. Hanaoka S, Masutani Y, Nemoto M et al (2017) Landmark-guided diffeomorphic demons algorithm and its application to automatic segmentation of the whole spine and pelvis in CT images. *Int J Comput Assist Radiol Surg* 12:413–430. <https://doi.org/10.1007/s11548-016-1507-z>
9. Brenner DJ, Hall EJ (2007) Computed tomography—an increasing source of radiation exposure. *N Engl J Med* 357:2277–2284. <https://doi.org/10.1056/NEJMr072149>
10. Yazici M, Acaroglu ER, Alanay A et al (2001) Measurement of vertebral rotation in standing versus supine position in adolescent idiopathic scoliosis. *J Pediatr Orthop* 21:252–256
11. Dubouset J, Charpak G, Dorion I et al (2005) A new 2D and 3D imaging approach to musculoskeletal physiology and pathology with low-dose radiation and the standing position: the EOS system. *Bull Acad Natl Med* 189:287–297 (**discussion 297–300**)
12. Humbert L, De Guise JA, Aubert B et al (2009) 3D reconstruction of the spine from biplanar X-rays using parametric models based on transversal and longitudinal inferences. *Med Eng Phys* 31:681–687. <https://doi.org/10.1016/j.medengphy.2009.01.003>

13. Ilharreborde B, Steffen JS, Nectoux E et al (2011) Angle measurement reproducibility using EOS three-dimensional reconstructions in adolescent idiopathic scoliosis treated by posterior instrumentation. *Spine* 36:E1306–E1313. <https://doi.org/10.1097/BRS.0b013e3182293548>
14. Carreau JH, Bastrom T, Petcharaporn M et al (2014) Computer-generated, three-dimensional spine model from biplanar radiographs: a validity study in idiopathic scoliosis curves greater than 50 degrees. *Spine Deform* 2:81–88. <https://doi.org/10.1016/j.jspd.2013.10.003>
15. Ferrero E, Lafage R, Vira S et al (2016) Three-dimensional reconstruction using stereoradiography for evaluating adult spinal deformity: a reproducibility study. *Eur Spine J*. <https://doi.org/10.1007/s00586-016-4833-5>
16. Kadoury S, Chretien F, Labelle H (2009) Personalized X-ray 3-D reconstruction of the scoliotic spine from hybrid statistical and image-based models. *IEEE Trans Med Imaging* 28:1422–1435. <https://doi.org/10.1109/TMI.2009.2016756>
17. Moura DC, Barbosa JG (2014) Real-scale 3D models of the scoliotic spine from biplanar radiography without calibration objects. *Comput Med Imaging Graph* 38:580–585. <https://doi.org/10.1016/j.compmedimag.2014.05.007>
18. Lecron F, Boisvert J, Mahmoudi S et al (2013) Three-dimensional spine model reconstruction using one-class SVM regularization. *IEEE Trans Biomed Eng* 60:3256–3264. <https://doi.org/10.1109/TBME.2013.2272657>
19. Aubert B, Vidal PA, Parent S et al (2017) Convolutional neural network and in-painting techniques for the automatic assessment of scoliotic spine surgery from biplanar radiographs. In: *Medical image computing and computer-assisted intervention—MICCAI 2017*. Springer, Cham, pp 691–699
20. Barrey C, Jund J, Noseda O, Roussouly P (2007) Sagittal balance of the pelvis-spine complex and lumbar degenerative diseases. A comparative study about 85 cases. *Eur Spine J* 16:1459–1467. <https://doi.org/10.1007/s00586-006-0294-6>
21. Lafage V, Schwab F, Skalli W et al (2008) Standing balance and sagittal plane spinal deformity: analysis of spinopelvic and gravity line parameters. *Spine* 33:1572–1578. <https://doi.org/10.1097/BRS.0b013e31817886a2>
22. Canavese F, Turcot K, De Rosa V et al (2011) Cervical spine sagittal alignment variations following posterior spinal fusion and instrumentation for adolescent idiopathic scoliosis. *Eur Spine J* 20:1141–1148. <https://doi.org/10.1007/s00586-011-1837-z>
23. Rousseau M, Laporte S, Chavary-bernier E et al (2007) Reproducibility of measuring the shape and three-dimensional position of cervical vertebrae in upright position using the EOS stereoradiography system. *Spine* 32:2569–2572. <https://doi.org/10.1097/BRS.0b013e318158cba2>
24. Lüthi M, Gerig T, Jud C, Vetter T (2018) Gaussian process morphable models. *IEEE Trans Pattern Anal Mach Intell*. <https://doi.org/10.1109/tpami.2017.2739743>
25. Ebrahimi S, Angelini E, Gajny L, Skalli W (2016) Lumbar spine posterior corner detection in X-rays using Haar-based features. In: *2016 IEEE 13th international symposium on biomedical imaging (ISBI)*, pp 180–183

## Affiliations

Laurent Gajny<sup>1</sup>  · Shahin Ebrahimi<sup>1</sup>  · Claudio Vergari<sup>1</sup>  · Elsa Angelini<sup>2,3</sup>  · Wafa Skalli<sup>1</sup> 

<sup>1</sup> Institut de Biomécanique Humaine Georges Charpak, Arts et Métiers ParisTech, 151 boulevard de l'Hôpital, 75013 Paris, France

<sup>2</sup> LTCI, Telecom ParisTech, Université Paris-Saclay, Paris, France

<sup>3</sup> ITMAT Data Science Group, NIHR Imperial BRC, Imperial College London, London, UK